Late Pleistocene to Holocene palaeoenvironmental variability in the NW Spanish mountains: insights from a source-to-sink environmental magnetic study of Lake Sanabria

VIOLETA BORRUEL-ABADÍA[1,2], MIRIAM GÓMEZ-PACCARD[3,4], JUAN C. LARRASOAÑA[1,3,*], MAYTE RICO[5], BLAS VALERO-GARCÉS[5], ANA MORENO[5], MARGARITA JAMBRINA-ENRÍQUEZ[6], RUTH SOTO[1]

[1] Instituto Geológico y Minero de España, Unidad de Zaragoza, Manuel Lasala 44, 9B, 50006 Zaragoza, Spain.

[2] Instituto de Geociencias (CSIC-UCM), C/ José Antonio Novais 12, 28040 Madrid, Spain

[3] Institute of Earth Sciences Jaume Almera (ICTJA-CSIC), Lluís Solé i Sabarís s/n, 08028 Barcelona, Spain

[4] Géosciences Rennes, UMR 6118, Université de Rennes 1, Campus de Beaulieu 35042 Rennes Cedex, France

[5] Instituto Pirenaico de Ecología (IPE-CSIC), Avda. Montañana 1005, 50059 Zaragoza, Spain

[6] Departamento de Geología, Universidad de Salamanca, Plaza de los Caídos s/n, 37008 Salamanca, Spain

[*] *Corresponding author: Tel.:* +34 934095410, *E-mail:* jc.larra@igme.es

Abstract

We present a source-to-sink environmental magnetic study of a sediment core from Lake Sanabria (NW Iberian Peninsula) and rocks of its catchment. Our results indicate the occurrence of magnetite, and likely also pyrrhotite, in sediments accumulated between ca 26 and 13 cal ka BP in a proglacial lake environment. These minerals

appear to dominate also the magnetic assemblage of Paleozoic rocks from the lake catchment. This indicates that sedimentation was then driven by the erosion of glacial flour, which suffered minimal chemical transformation due to a rapid and short routing to the lake. A sharp change in magnetic properties observed in the lake sediments between 13 and 12.6 cal ka BP reflects the rapid retreat of glaciers from the lake catchment. Sediments from the upper half of the studied sequence, accumulated after 12.6 cal ka BP in a lacustrine environment with strong fluvial influence, contain magnetite and smaller amounts of maghemite and greigite. We interpret that greigite grew authigenically under anoxic conditions caused by enhanced accumulation of organic matter into the lake. The occurrence of maghemite in these sediments suggests pedogenic activity in the then deglaciated lake catchment prior to the erosion and transportation of detrital material into the lake.

Keywords: Lacustrine sediments; Environmental Magnetism; Deglaciation, Iberian Peninsula.

1. Introduction

The sedimentary record of lakes is one of the best archives for reconstructing past environmental and climatic changes in continental regions because: i) they are typically characterized by a continuous sedimentation, which contrast with the fragmentary nature of most continental records; ii) they often have high accumulation rates, which enables detection of paleoenvironmental changes at even down to decadal timescales; iii) they usually have a good spatial representation, which makes possible to obtain widely distributed paleoclimatic records; and iv) they are very sensitive to hydrological

variations in the watershed, which are one of the most dramatic manifestations of Holocene and future climate change (Dergachev *et al*., 2007; Giorgio and Lionello, 2008). Because of their sensitivity, mountain lakes are excellent sensors to environmental and climatic changes, and their sediment records can be used to infer high-temporal resolution paleoenvironmental reconstructions applying different techniques and proxies. One of the most important issues faced when studying climate variability in lake records is the development of parameters that can be used as reliable proxies for the different environmental processes that affect lakes and their catchments. The most successful approach developed so far has been that obtained from multi-proxy datasets, because it enables the co-record of climate variability on the basis of different physical, chemical or biological processes (Last and Smol, 2001).

In this context, environmental magnetic techniques have made an important contribution to these multi-proxy datasets because they are cheap, non destructive, and enable the characterization of lacustrine sediments and the reconstruction of the environmental history in lake catchment areas through its impact in the type, concentration and grain size of magnetic minerals. Such minerals are ubiquitous in most lake sediments, and they are very sensitive to even minor changes in the physical and chemical conditions prevailing during sedimentation and diagenesis (Evans and Heller, 2003; Liu *et al.*, 2012; Oldfield, 2013). However, an accurate interpretation of the paleoenvironmental significance of rock magnetic properties of lacustrine sediments requires a good knowledge of the magnetic properties of rocks of the catchment area of the lake. Although this approach seems obvious and have been followed in some instances (Dearing *et al.*, 2001; Rosenbaum and Reynolds, 2004), detailed rock-magnetic studies of both catchment rocks and lacustrine sediments are not routinely conducted (see Liu *et al.*, 2012; Oldfield, 2013).

Here, we present a source-to-sink environmental magnetic study of lacustrine sediments cored from Lake Sanabria (Zamora, NW Spain), which constitutes a unique archive of climatic changes during the Upper Pleistocene and the Holocene in the mountains of the northwest Iberian Peninsula (Fig. 1). This approach has enabled identification of the main physico-chemical processes that control the production of sedimentary load in the catchment and its possible modifications once accumulated in the lake. A comparison of our environmental magnetic data with sedimentological, geochemical and chronological data previously published for the same core (Jambrina-Enríquez *et al.*, 2014) provide new insights on past paleoenvironmental changes occurred in the catchment of the lake in response to climate variability during the Late Pleistocene and the Holocene.

2. Geological and geomorphological setting

Lake Sanabria (42º07′30'' N, 06º43′00'' W, 1000 m a.s.l.) is located in the NW Spanish mountains in the province of Zamora, and constitutes the largest lake of glacial origin in the Iberian Peninsula (Aldasoro *et al.*, 1991; de Hoyos, 1996; Vega *et al.*, 1992), (Fig. 1). The lake basin is bounded by a terminal moraine developed during the regional last glaciation, is elongated along an E-W direction, and is characterized by two subbasins developed under the areas of former maximum ice accumulation and over-deepening (Vega *et al.*, 1991; Vega *et al.*, 2005; Jiménez-Sánchez *et al.*, 2012; Rodríguez-Rodríguez *et al.*, 2014). The eastern and western subbasins have maximum depths of 51 m and 45 m, respectively, and are separated by a central ridge located 20 m below the lake surface (Vega et al., 2005). Lake Sanabria is a warm (4.5-24.8ºC water temperature), oligotrophic and meromictic lake characterized by oxygenated conditions

100 of the whole water column throughout the year (de Hoyos, 1996; de Hoyos *et al.*, 1998;
101 de Hoyos and Comin, 1999).

102 The lake lies in an exorheic drainage basin that extends over an area of 127 km^2 (Fig.
103 1). The Tera River is the main source of water and sediment input to the lake, and
104 constitutes also its main outlet. This river drains the Segundera and Cabrera mountain
105 ranges, which constitute the northern and central part of the lake catchment (Fig. 1).
106 These ranges are characterised by a flat morphology at elevations between 1600 and
107 2000 m a.s.l. and by peaks that reach up to 2128 m a.s.l. The southern part of the lake
108 catchment has a lower relief (highest peaks of up to 1844 m a.s.l.), and is drained by
109 two tributaries of the Tera River (Cardena and Segundera rivers). The region is located
110 in the transition between Mediterranean and Atlantic climates (de Hoyos 1996, Giralt *et*
111 *al.* 2011). Water input into the lake is strongly linked to precipitation in the watershed,
112 which averages 1400 mm/year and is mainly related to the passage of Atlantic fronts
113 during the winter and spring months. The high uplands and peaks remain mostly snow-
114 covered from December to March. Temperatures are low in winter (monthly average
115 below 4ºC between November and May) and high (maximum 36ºC) during the summer.
116 The catchment of the lake is covered by *Quercus pyrenaica* woodland with patches of
117 *Pinus sylvestris, Juniperus oxycedrus, Taxus baccata,* and *Ilex aquifolium* (Vega *et al*
118 1992, Julià *et al.* 2007, Jambrina-Enríquez *et al.*, 2014). This vegetation is replaced with
119 pastures and shrubs above 1700 m a.s.l. (Vega *et al.* 1992, Juliá *et al.* 2007). *Populus*
120 *nigra, Alnus glutinosa, Fraxinus angustifolia, Salix sp., and* aquatic macrophytes
121 dominate the lake shore vegetation. The phytoplancton community of the lake is
122 composed of Cryptophyta, Chlorophyta, Cyanobacteria and less abundant diatoms (de
123 Hoyos, 1996; de Hoyos and Comin 1999, Negro *et al.* 2000). Lake productivity is

124 highly sensitive to the rainfall regime and consequently is greatly influenced by the
125 North Atlantic Oscillation (NAO) (de Hoyos, 1996; Giralt *et al*., 2011).

126 The catchment of Lake Sanabria is made up of granitic and metamorphic Paleozoic
127 rocks originated during the Variscan Orogeny (Martínez-García, 1973; Vega and
128 Aldaroso, 1994; Pérez-Estaún and Bea, 2004) (Figs. 1 and 2). The central part of the
129 catchment is occupied by glandular gneisses of the Ollo de Sapo Formation, which
130 hosts several granitic bodies (Pérez-Estaún and Bea, 2004). Both granites and gneiss are
131 coarse grained and include quartz and plagioclase phenocrystals of up to 4 cm long (Fig.
132 2c-f). The northern part of the catchment is made up of schists and quartzites of the
133 Puebla Formation and tuffs of the Ollo de Sapo Formation. Quartzites and tuffs include
134 a dominant coarse-grained fraction (sand and microconglomerate) (Fig. 2g). Schists of
135 the Puebla Formation are the only fine-grained dominated rocks in the catchment of
136 Lake Sanabria (Pérez-Estaún and Bea, 2004) (Fig. 2a, b).

137 Geomorphological evidence indicates three main glacial pulses in the catchment of
138 Lake Sanabria since the latest Pleistocene (Vega *et al*., 2005; Cowton *et al*., 2009;
139 Rodríguez-Rodríguez *et al*., 2011; Jiménez-Sánchez *et al*., 2012). The first and most
140 extensive pulse was characterized by a large plateau ice cap, which covered an area of
141 more than 440 km^2 and formed by the coalescence of three glaciers descending from the
142 Tera, Segundera, and Cardena valleys (Fig. 1). This ice cap was drained by a large
143 outlet glacier that reached an altitude as low as 1000 m (Cowton *et al*., 2009), and
144 resulted in the accumulation of extensive till deposits at >1500 m a.s.l. (Fig. 2h) and in
145 the formation of the terminal moraine complex east of Lake Sanabria. Ages for the
146 regional maximum glacier extent in the region and in the neighbouring Cantabrian
147 Range (Jiménez-Sánchez *et al*., 2002; Moreno *et al*., 2010; Jalut *et al*., 2010; Jiménez-
148 Sánchez *et al*., 2012) point to a maximum ice extent prior to the Last Glacial Maximum

149 (LGM), and a complex evolution with a glacier readvance during the LGM as indicated
150 by cosmogenic dating of some boulders of the terminal moraine (Rodríguez-Rodríguez
151 *et al*., 2014), and two more reduced glacial pulses of uncertain age (Cowton *et al*.,
152 2009) that led to the formation of small moraines in the high uplands and the highest
153 cirques (Fig. 1).

154 The recent recovery of sedimentary cores from different locations within Lake
155 Sanabria and their paleolimnological study has enabled implementation and refinement
156 of the geomorphic evolution of the lake catchment (Rodríguez-Rodríguez *et al*., 2011;
157 Jambrina-Enríquez *et al*., 2014). The recovered sediments are made of (i) clastic, sandy
158 and silty facies, (ii) organic matter-rich silts and oozes, and (iii) clastic-organic silts and
159 oozes. Based on sedimentologic and geochemical data, these studies have separated the
160 sedimentary record of Lake Sanabria into three main lithological units (see Jambrina-
161 Enríquez *et al*., 2014 for more details):

162 -*Unit 3* (890 to 729 cm depth, >25.5-13.9 cal ka BP) is composed of a clastic
163 association including dm-thick massive to slightly banded light greenish gray fine to
164 medium silt and cm to dm- thick massive sand in lenses and irregular pockets some
165 with iron oxides. These sediments accumulated in a proglacial environment at the
166 eastern subbasin of Lake Sanabria between > 25.5 cal ka BP and 13.9 cal ka BP. The
167 occurrence of proglacial sediments before 25.5 cal ka BP indicates that the Tera glacial
168 retreated before the global LGM (Rodríguez-Rodríguez *et al*., 2011; Jambrina-Enríquez
169 *et al*., 2014) to create the Lake Sanabria Basin. No clear evidence of erosion during the
170 global LGM glaciar readvance (Rodríguez-Rodríguez *et al*., 2014) has been found in
171 sediments from this unit.

-*Unit 2* (729 to 670 cm depth, 13.9-11.2 cal ka BP) is a transitional unit with an organic-clastic facies association. Subunit 2C (729-713 cm depth, 13.9-13.0 cal ka BP) and subunit 2A (701-670 cm depth, 12.4-11.2 cal ka BP) are more organic, and subunit 2B (713 to 701 cm depth, 13.0-12.4 cal ka BP) is a fining upward sequence of grey sand and sandy silt. During this period, geochemical and sedimentological evidences indicate that glaciers were restricted to the higher parts of the catchment of the lake, with the exception of a short period of glacier advance around 13 cal ka BP (Jambrina-Enríquez *et al*., 2014) that likely resulted in the formation of moraines in the high uplands.

- *Unit 1* (670-0 cm, 11.2-0.81 cal ka BP) comprises an organic facies association and represents deposition in the distal areas of the lake with variable fluvial influence. Five subunits (from 1E to 1A) have been defined according to the relative occurrence of clastic intercalations (see Jambrina-Enríquez *et al*., 2014 for more details). These sediments accumulated in a fluvio-lacustrine environment after 11.2 cal ka BP and throughout the Holocene.

3. Materials and methods

3.1. Studied core and previous paleolimnological data

Core SAN04-3A-1K is the longest of the sediment cores available from Lake Sanabria. It was recovered in May 2004 from the deeper eastern sub-basin of the lake (Fig. 1) using a Kullenberg platform and coring equipment recovered (Jambrina-Enríquez *et al*., 2014). The core was immediately sealed and stored in a cold room at +4ºC, and was subsequently studied following the protocol recommended by the Limnological Research Centre (LRC) from the University of Minnesota (Minneapolis, USA) (Schnurrenberger *et al*., 2003). A multiproxy sedimentological, geochemical and

196 biological dataset for core SAN04-3A-1K has been published recently by Jambrina-
197 Enríquez *et al*. (2014). From this dataset, we have selected elemental abundances and
198 total carbon (TC) and nitrogen (N) contents for comparison with our rock magnetic
199 results. In this setting, inorganic is below detection limit, so TC measurements actually
200 represent the TOC (Jambrina-Enríquez *et al*. 2014). With regards to elemental
201 abundances, we have used the elemental ratio Rb/Zr as an indicator of relative grain size
202 changes through core SAN04-3A-1K. Rb is typically associated with clay minerals and
203 micas, and therefore tends to be enriched in the relatively finer-grained fraction in
204 siliciclastic sediments. Zr is typically enriched in heavy minerals and is commonly
205 associated with the relatively coarser-grained fraction in siliciclastic sediments (Dypvik
206 and Harris, 2001). Higher Rb/Zr values therefore can be taken to indicate finer grain
207 sizes (Dypvik and Harris, 2001). Finally, we have used the C/N atomic ratio to
208 determine the relative importance of aquatic versus terrestrial vegetation. The reader is
209 referred to Jambrina-Enríquez *et al.* (2014) for details on the methodology employed to
210 obtain this dataset, and also for details on the chronological model available for core
211 SAN04-3A-1K.

212 Light coloured silts that made up most of Unit 3 are characterized by low TOC and
213 C/N ratios, and by high Rb/Zr ratios (Fig. 3). This attests to deposition of an organic-
214 poor, fine-grained material that is interpreted as a rock flour derived from glacial
215 grinding throughout the then ice-covered catchment of Lake Sanabria. The occasional
216 dm-thick lenses of sand embedded in this unit are characterized by higher C/N and
217 lower Rb/Zr ratios (Fig. 3). This indicates the input of coarser grained material and
218 allochtonous organic matter into the lake, probably in response to decreased grinding
219 activity during transient periods of glacier retreat and incipient establishment of
220 vegetation in some areas of the catchment, likely associated to increased meltwater

fluxes and higher transport energy by glacier-fed rivers. Sediments from Unit 2 show an overall decrease in Rb/Zr ratios, which indicate a coarsening of the detrital material arriving to the lake. TOC values also increase upward in the unit in parallel with fluctuating, but overall higher C/N ratios, as compared with sediments of Unit 3. This indicates a larger input of organic matter derived from erosion of terrestrial vegetation, which is consistent with the occurrence of plant remains in the sediments. These data suggest rapidly decreasing glacier activity and a concomitant increase in the amount of vegetation in the catchment of the lake during deposition of Unit 2. Sediments of Unit 1 are characterized by high TOC values ranging between 5 and 13%, and by stable high C/N and low Rb/Zr ratios of ~12 and 0.4, respectively (Fig. 3). These properties are indicative of a widespread vegetation cover throughout the lake catchment and of the dominance of organic and clastic sedimentation in the lake, with the occasional input of coarser detrital material to the lake during discrete flooding episodes. This, coupled with sedimentological evidence for fluvial-originated processes (e.g. graded fining-upward sequences), points to the lack of glacier activity in the catchment of the lake and to sedimentation in a lacustrine environment with strong influence by the Tera River.

3.2. Environmental magnetism

Samples for environmental magnetic analyses were obtained by pushing 428 plastic boxes (2x2x2 cm) continuously into the working half of core SAN04-3A-1K. Additionally, 35 block samples corresponding to representative lithologies of the catchment area, including Paleozoic gneisses, graniodiorites, schists, quartzites and tuffs and Quaternary till, were collected (Fig. 1 and 2). Environmental magnetic analyses include measurements of the low field mass-specific magnetic susceptibility (χ), the

245 anhysteretic remanent magnetization (ARM) and two isothermal remanent
246 magnetizations (IRM) that were imparted at 0.1 T ($IRM_{0.1\ T}$) and 1.2 T (SIRM). χ was
247 measured with a Kappabridge KLY-2 (Geofyzica Brno) susceptibility bridge using a
248 field of 0.1 mT at a frequency of 470 Hz. AF demagnetization and ARM experiments
249 were conducted using a D-Tech 2000 (ASC Scientific) AF demagnetizer. The ARM
250 was applied along the Z axis of the samples with a dc bias field of 0.05 mT parallel to a
251 peak AF of 100 mT. $IRM_{0.1\ T}$ and SIRM were imparted using an IM10–30 pulse
252 magnetizer (ASC Scientific). In order to identify the main magnetic carriers contained
253 in our samples, thermal demagnetization of a three-axes IRM imparted at fields of 1.2,
254 0.3 and 0.1 T on 21 samples (14 lacustrine sediment samples and 7 block samples) was
255 conducted following the method of Lowrie (1990). Before the thermal treatment, the
256 lake and till samples were consolidated using sodium silicate and a non-magnetic
257 cement inside plastic boxes. After consolidation, the faces of the plastic boxes were cut
258 with a saw to extract the samples. Magnetizations were measured using a SRM755R
259 three axis cryogenic superconducting rock magnetometer (2G Enterprises). All these
260 measurements were performed at the Palaeomagnetic Laboratory of the Institute of
261 Earth Sciences Jaume Almera (CCiTUB-CSIC) in Barcelona, Spain. Further insights
262 into the magnetic mineralogy of the studied sediments and catchment rocks were
263 provided by variations of the magnetic susceptibility from room temperature to 700°C
264 and back to room temperature. These experiments were conducted (with an argon flow)
265 using a KLY-3S-CS3 (Agico Inc.) with a field intensity of 0.38 mT and 875 Hz of
266 operating frequency at the Magnetic Fabric Laboratory of the University of Zaragoza.

267 We have used different magnetic properties and interparametric ratios to determine
268 relative variations in the type, concentration, and grain size of magnetic minerals (Evans
269 and Heller, 2003; Peters and Dekkers, 2003). Mass-specific magnetic susceptibility (χ)

has been used as a first order indicator for the concentration of magnetic (s.l.) minerals. The S-ratio (defined as $IRM_{0.1T}$/SIRM; Bloemendal *et al*., 1992) has been used to detect changes in the relative concentration of low and high coercivity magnetic minerals. Then, the ARM and the "hard" IRM (HIRM, defined as SIRM-$IRM_{0.1T}$; Thompson and Oldfield, 1986) have been used as a proxy for the concentration of relatively low- and high- coercivity magnetic minerals, respectively. Finally, the SIRM/χ and χ_{ARM}/SIRM (being χ_{ARM} the mass-normalized ARM per unit bias field) ratios have been used to detect downcore changes in magnetic grain size (Thompson and Oldfield, 1986; Peters and Dekkers, 2003; Oldfield, 2013). All magnetic properties have been normalized by the dry weight of the samples.

4. Results

4.1. Magnetic properties of core SAN04-3A-1K sediments

ARM and HIRM data indicate rather constant concentrations of low- and high-coercivity minerals, respectively, throughout the core (Fig. 3). The only exceptions are two intervals at 125-225 and 600-700 cm deep (Fig 3), where ARM and HIRM experience a significant increase. Mass-specific magnetic susceptibility (χ) data are consistent with these variations inferred from ARM and HIRM, although in this case rather constant magnetic mineral abundances are also inferred for the interval at 600-700 cm deep (Fig. 3). S-ratios display low values between 0.6 and 0.7 through Unit 3, which is also characterized by the lowest ARM and HIRM values of the studied sequence (Fig. 3). This indicates minimum concentrations of both high- and low-coercivity minerals during deposition in proglacial conditions, although high-coercivity minerals are relatively dominant. Some of the massive sand lenses (e.g., at 810 cm) are

294 characterized by S-ratios as low as 0.5, which suggests a dominance of high-coercivity
295 minerals during periods of transient glacier retreat. S-ratios as low as ~0.6 are found in
296 the lowest part of Unit 2 coinciding with enhanced TOC and C/N ratios and decreased
297 Rb/Zr ratios, which again relates the dominance of high coercivity minerals with
298 decreased glacial activity in the lake catchment. S-ratios then experience a rapid shift
299 till clearly exceeding 0.9 at the top of Unit 2. This change is accompanied by a subtle
300 and more gradual increase in ARM and HIRM, which indicates that decreased glacial
301 activity during deposition of the upper half of Unit 2 was accompanied by a shift
302 towards slightly higher concentrations of both low- and high coercivity minerals and
303 towards a relative dominance of the former. Unit 1 shows stable S-ratios between 0.8
304 and 0.9, which indicates a sustained dominance of low-coercivity minerals throughout
305 the rest of the sequence, when sedimentation occurred under fluvio-lacustrine
306 conditions. ARM and HIRM values fluctuate in parallel throughout Unit 1, and are only
307 above background values coinciding with higher S-ratios in the lower part of Unit 1 and
308 the uppermost 2.5 m of the sequence (Fig. 3). Especially distinctive are the high ARM
309 and HIRM values found around 150 and 200 cm, which are separated by a clear
310 minimum in both parameters at around 170 cm and a distinctive low S-ratio of ~0.7.
311 Other remarkable features within Unit 1 are two short-lived minima in S-ratios at
312 around 545 and 640 cm, which correspond to two detrital layers characterized by
313 relative minima in TOC and higher than background Rb/Zr ratios (Fig. 3).

314 Variations in magnetic properties with sedimentary environments are further
315 illustrated in a plot that relates S-ratios versus ARM values (Fig. 4). Thus, sediments
316 accumulated under pro-glacial (Unit 3) and fluviolacustrine (Unit 1) conditions form
317 two distinctive clusters characterized by S-ratios<0.75 and ARM<2 x 10^{-6} Am^2/kg (Unit
318 3) and S-ratios>0.75 and ARM>2 x 10^{-6} Am^2/kg (Unit 1). Sediments from the lower

319 half of Unit 2 cluster around those of Unit 3, whereas those from its upper half cluster
320 with sediments from Unit 1, thereby marking a decreasing influence of glacial activity
321 during their sedimentation. With respect to variation in χ_{ARM}/SIRM ratios, which are
322 typically interpreted in terms of magnetic grain size, they change from values of ~0.3
323 10^{-3} mA^{-1} within Unit 3 and the lower half of Unit 2, to slightly larger values of ~0.6 10^{-3}
324 mA^{-1} in the upper half of Unit 2 and throughout the lower part of Unit 1, and to
325 highest values of ~1.5 10^{-3} mA^{-1} in the upper part of Unit 1 (Fig. 3). The stepwise
326 upward decrease in magnetic grain size indicated by χ_{ARM}/SIRM is consistent with
327 changes in SIRM/χ ratios, although relatively finer grain sizes are also indicated in the
328 transition from Units 2 to 1 (e.g., highest values of ~10-20 k Am^{-1}; Fig. 3). The link
329 between sedimentary facies and magnetic grain sizes is also readily visible in a plot of
330 S-ratio versus SIRM/χ (Fig. 4b). Sediments accumulated under the influence of glacial
331 activity (Unit 3 and lower part of Unit 2) are characterized by distinctively lower S-
332 ratios (<0.75) and lower SIRM/χ values (<2 k Am^{-1}; coarser magnetic grain sizes),
333 whereas those accumulated mainly under fluviolacustrine conditions (upper part of Unit
334 2 and Unit 1) display larger S-ratios (>0.75) and higher SIRM/χ values (2-20 k Am^{-1};
335 finer magnetic grain sizes).

336 Thermal demagnetization of a three-axis IRM of sediments from core SAN-04-3A-
337 1K indicates the complete demagnetization of the IRM below 590°C in all the studied
338 samples regardless of sediment type, thereby pointing to the occurrence of magnetite
339 throughout the whole studied sedimentary sequence (Fig. 5 g-j). Although the new
340 formation of new magnetic phases upon heating totally obscures some of the
341 thermomagnetic experiments (e.g., Fig. 6h), the main drop of magnetic susceptibility
342 below 590°C observed in most samples (Fig. 6f, g) supports the ubiquitous occurrence
343 of magnetite. χ_{ARM}/SIRM ratios reported in the core range between 0.3 and 1.5 10^{-3} mA^{-}

^{1} (Fig. 3), which is always lower than the value of 2 10^{-3} mA^{-1} that is typically regarded as indicative for magnetite grains produced by magnetotactic bacteria (Oldfield, 2013). These data therefore indicate that magnetite throughout the studied core is detrital in origin. A subtle inflection in the magnetic susceptibility of Unit 1 and the upper part of Unit 2 samples is observed in thermomagnetic experiments around 260°-280°C (Fig. 6f, g). Such inflection is commonly attributed to the thermal alteration of maghemite (Liu *et al.*, 2005), which appears to be present in Unit 1 and the upper part of Unit 2.

Thermal demagnetization of a three-axis IRM of samples from Unit 3 are characterized by an additional and progressive IRM drop below 350°C that is observed in the soft, intermediate and hard IRM components (Fig. 5j). This behavior might be attributed to the occurrence of either pyrrhotite (Larrasoaña *et al*., 2007) or, alternatively, maghemite (Liu *et al*., 2005). Thermomagnetic runs of samples from Unit 3 and the lower part of Unit 2 do not enable clear discrimination between these two minerals, whose distinctive features are obscured by new formation of large amounts of magnetite upon heating (Fig. 6h). Nevertheless, S-ratios lower than 0.8 throughout Unit 3 and the lower part of Unit 2 seem to be more consistent with pyrrhotite than with maghemite (given the overall lower coercivity of the later; Peters and Dekkers, 2003). Samples from the upper part of Unit 2 and Unit 1 have, in contrast, a marked IRM drop in IRM intensity below 250°C (Fig. 5g-i) that is consistent with the occurrence of greigite (Roberts *et al*., 2011). Greigite is not apparent in thermomagnetic runs (Fig. 6f, g), probably because its distinctive feature (a decrease in magnetic susceptibility around 300°C; Roberts *et al.*, 2011) is overlapped with thermal alteration of maghemite at about the same temperature. Nevertheless, SIRM/χ values throughout the upper part of Unit 2 and Unit 1, which range between 5 and 20 k Am^{-1} (Fig. 3), are consistent with the coexistence of greigite in these sediments along with magnetite (Oldfield, 2013).

369

370 **4.2. Magnetic properties of catchment rocks**

371 Paleozoic rocks from the catchment of Lake Sanabria have mean ARM values
372 ranging between 2.5 x 10^{-7} and 16.5 x 10^{-7} Am^2/kg, with virtually all samples displaying
373 values of <20 x 10^{-7} Am^2/kg (Fig. 4a). These rocks are also characterized by S-ratios
374 that are always lower than 0.75, with mean values oscillating between 0.65 and 0.49
375 (Fig. 4a). The lowest S-ratios, for both individual samples and their mean value,
376 correspond to tuffs from the Ollo de Sapo Formation. Overall, mean S-ratios and ARM
377 values of these Paleozoic rocks are both statistically identical to those of sediments from
378 Unit 3 and the lower part of Unit 2 (Fig. 4a). Quaternary tills, in contrast, display a large
379 variability in both S-ratios and ARM values. Some till samples have S-ratios and ARM
380 values that overlap with those of Paleozoic catchment rocks and of sediments from Unit
381 3 and the lower part of Unit 2. Other tills have S-ratios and ARM values that are much
382 closer to those of sediments from Unit 1 and the upper part of Unit 2 (Fig. 4a). With
383 regards to SIRM/χ values, both Paleozoic catchment rocks and Quaternary tills display
384 values similar to those of sediments from Unit 3 and the lower part of Unit 2 (Fig. 4b).
385 The only exceptions are three till and three schist samples, whose SIRM/χ ratios
386 overlap with those of sediments from Unit 1 and the upper part of Unit 2.

387 Thermal demagnetization results indicate that the IRM of tuffs, granites, schists and
388 gneisses from the catchment of Lake Sanabria is nearly completely destroyed below
389 590°C, which points to the occurrence of magnetite in these lithologies (Fig. 5a-d).
390 Magnetite appears to be the dominant magnetic mineral also in Quaternary till samples,
391 where the IRM disappears completely also below 590°C (Fig. 5e, f). Thermomagnetic
392 runs of Paleozoic catchment rocks and Quaternary tills do not enable clear identification

393 of magnetite due to the new formation of large amounts of magnetic minerals (mainly
394 magnetite) upon heating (Fig. 6a-e). An additional decrease in IRM intensity is
395 observed below 350°C in gneisses, granites, schists and some till samples (Fig. 5a, b, c,
396 f). Such decrease might be interpreted as resulting from the occurrence of pyrrotite
397 (Dekkers, 1989; Larrasoaña *et al*., 2007), but might be also attributed to the thermal
398 alteration of maghemite. Thermomagnetic data for schists, tuffs and some till samples
399 reveal a clear peak in magnetic susceptibility that begins at ~280°C, peaks at ~300°C,
400 and is followed by a smoother decrease (Fig. 6c-e). This peak is different to the slight
401 deflection attributed to the thermal alteration of maghemite (see Fig. 6f, g) (e.g., Liu *et*
402 *al*., 2005), but is more similar to what has been reported for some sedimentary greigite
403 (see Roberts *et al*., 2011) as well as for some sedimentary (Horng and Roberts, 2006)
404 and some synthetic (O'Reilly *et al*., 2000) pyrrhotite-bearing samples. Pyrrhotite is a
405 magnetic iron sulfide whose occurrence in plutonic and metamorphic rocks is expected,
406 as opposed to greigite (Dunlop and Özdemir, 1997; Liu *et al*., 2012). Thus, although
407 rock magnetic evidence is not fully conclusive, we interpret that pyrrhotite (rather than
408 greigite) is also present in Paleozoic rocks (and Quaternary tills derived from them)
409 from the catchment of Lake Sanabria in addition to magnetite, which dominates the
410 magnetic assemblage.

411

412 **5. Discussion**

413 **5.1. Origin of magnetic minerals in core SAN-04-3A-1K sediments**

414 Our rock magnetic study evidences the occurrence of two main magnetic
415 assemblages in the lake sediments that are closely related to sedimentary environments
416 prevailing during their deposition. Rock magnetic results indicate that the magnetic

assemblage of most rocks from the catchment of Lake Sanabria and of sediments accumulated under the influence of glacial activity (e.g. Units 3-2C) is dominated by magnetite, with a smaller contribution of (likely) pyrrhotite. Bulk magnetic properties of these sediments and of catchment rocks are statistically undistinguishable. Overall, these results indicate that both magnetite and pyrrhotite in these sediments are best interpreted as detrital minerals sourced in catchment rocks of Lake Sanabria and accumulated into the lake. Magnetite is the most common magnetic mineral found in plutonic and metamorphic rocks such as those cropping out in the catchment of Lake Sanabria (Dunlop and Özdemir, 1997). Magnetite is an iron oxide that is stable under oxic conditions prevailing during weathering and transport in continental settings; therefore, its presence as a detrital mineral in the studied sediments conforms to previous expectations. The occurrence of pyrrhotite as a detrital mineral in sediments of Units 3 and 2C is problematic, however, because pyrrhotite is an iron sulfide that is highly unstable under oxic conditions prevailing during weathering and transportation. For it to be present as a detrital mineral, a rapid transport mechanism minimizing oxidation is required (Horng and Roberts, 2006). We interpret that rapid transport of a glacial flour by subglacial meltwaters, channelized through the frequent subglacial Nye scours appearing in the catchment of the lake (Cowton *et al*., 2009), enabled preservation of pyrrhotite during its transport to the lake. Glacial conditions provide also below freezing temperatures that might have driven chemical alteration reactions to a minimum, further favoring preservation of pyrrhotite. The probable occurrence of pyrrhotite in at least some till samples (e.g., Fig. 5f, 6e) appears to attest for its transit from the source rocks in the catchment to the sink in the lake basin via glacial-related processes.

441 Rock magnetic results indicate that the magnetic assemblage of sediments
442 accumulated in fluviolacustrine environments, without the influence of glacial activity
443 (e.g. Units 1 and 2B-A), is dominated by magnetite and includes also variable amounts
444 of greigite (as indicated by SIRM/χ ratios, Fig. 3) and maghemite (as indicated by
445 thermomagnetic runs, Fig. 6f, g). The bulk magnetic properties of these sediments
446 clearly depart from those of the main catchment rocks (Fig. 4). These results point to a
447 different origin for the magnetic assemblage in these sediments, which involved a shift
448 towards a lower coercivity (e.g. larger S-ratios) and towards larger concentrations of
449 magnetic minerals (e.g. larger ARMs). Greigite is a magnetic iron sulfide that is often
450 reported in lake sediments, where sulfate reduction triggers dissolution of detrital
451 magnetic minerals and favors authigenic growth of greigite as an intermediate product
452 in the pyrite formation pathway (e.g. Snowball, 1991; Roberts *et al*., 2011; Liu *et al*.
453 2012; Oldfield, 2013). Greigite formation is favored when sulfide is produced in low
454 amounts (Roberts and Weaver, 2005), which is typical for small lakes due to the low
455 availability of dissolved sulfate in lake waters. The occurrence of greigite in sediments
456 of Units 2B-A and 1, but not in the catchment rocks, points to a diagenetic origin of this
457 mineral in these sediments. Since the whole water column of Lake Sanabria is oxic
458 throughout the year (De Hoyos, 1996), we interpret that sulfate-reducing conditions
459 leading to authigenic growth of greigite were driven by accumulation of terrestrial
460 organic matter within the sediments. SIRM/χ ratios indicate that formation of greigite
461 appears to have started towards the base of Subunit 2B, when TOC reached a threshold
462 ~5%, and then continued throughout the rest of the sequence but specially around the
463 transition from Units 2A and 1E and the uppermost 2.5 m of the studied core (Fig. 3). It
464 seems, however, that diagenetic conditions alone cannot explain the magnetic
465 assemblage of these fluvio-lacustrine sediments. Thus, the occurrence of some

maghemite in these sediments suggests pedogenic activity in the lake catchment prior to the transport of detrital material into the lake (see Liu *et al*., 2012; Oldfield, 2013). ARM values of some till samples, well above those of catchment rocks (Fig. 4a), support the authigenic growth of maghemite and its subsequent transport into the lake. Maghemite is an unstable magnetic mineral under reducing conditions. Its preservation within sediments accumulated without the influence of glacial activity (Units 1 and 2B-A) therefore suggests only mild reducing conditions.

Concerning grain size-dependent parameters, they demand a cautious interpretation due to the different mineral magnetic assemblages found throughout the core. The rather constant SIRM/χ values of <1 kA/m for sediments of Units 3 and 2C are very similar to individual samples from different rock types from the lake catchment (see Fig. 4). We interpret that glacial processes led to an effective mixing of detrital components within the glacial flour that was transported into the lake basin. Sediments from Units 2B to 1 have SIRM/χ values of >3 kA/m that are distinctively larger than those of most rock types from the lake catchment, which points to finer magnetic grain sizes. Such smaller magnetic grain sizes might be linked to the occurrence of detrital maghemite of pedogenic origin or to authigenic formation of greigite, which are in both cases typically fine grained (e.g. Roberts *et al*., 2011; Liu *et al*., 2012).

5.2. Paleoclimatic implications

The magnetic properties of lake sediments depend on the relative importance of different processes that, operating both in the catchment and in the lake itself, influence the composition, concentration, and grain size of magnetic minerals (Liu *et al*., 2012; Oldfield, 2013). The magnetic assemblage of sediments from Units 3 and 2C of core

490 SAN-04-3A-1K is characterized by detrital magnetite and (probably also) pyrrhotite,
491 which indicates minimal mineralogical transformation in response to a rapid transport of
492 detrital material into the lake basin via glacial-related processes. The magnetic
493 assemblage of sediments from Units 2B to 1 is characterized by the occurrence of
494 detrital magnetite, with smaller contributions from authigenic greigite and detrital
495 maghemite. This indicates a digenetic overprint once the sediments were accumulated
496 in the lake, but also a significant imprint of pedogenic activity in the catchment before
497 detrital material was transported into the lake. The transition between these two
498 distinctive magnetic assemblages in the sedimentary sequence of Lake Sanabria is
499 rather abrupt, and therefore indicates a very rapid change from an initial period in which
500 glacial activity dominates throughout the lake catchment to a period in which pedogenic
501 processes take the lead following deglaciation. Our rock magnetic study therefore
502 provides an independent validation for the rapid deglaciation of the Lake Sanabria
503 catchment deduced from sedimentological and geochemical data (Jambrina-Enríquez *et*
504 *al*., 2014).

505 Implementation of the multiproxy dataset available for sediments from core SAN-04-
506 3A-1K (Jambrina-Enríquez *et al*., 2014) with rock-magnetic data enables refinement of
507 the paleoenvironmental evolution of the Lake Sanabria basin during the last glacial
508 cycle (Fig. 7). Due to uncertainties in the age model in the lower part of the record,
509 which is constrained only by two radiocarbon dates at 25.6 and 14.5 cal ka BP,
510 paleoclimatic inferences prior to 14.5 cal ka BP need to be treated with caution. Highest
511 Rb/Zr ratios and lowest TOC and C/N values between 26 and 20 cal ka BP (e.g. lower
512 part of Unit 3) indicate widespread production of glacial flour and the lack of vegetation
513 cover in the lake catchment during oxygen isotopic stage (OIS3) and most of the LGM.
514 Lowest ARM values and low S-ratios during this period, identical to those of the

515 catchment rocks, indicate negligible mineralogical transformation during transport and
516 deposition of glacial-derived sediments. Coupled with geomorphological evidence
517 (Rodríguez-Rodríguez *et al*., 2011, 2014), these data indicate full-glaciated conditions
518 in the catchment of Lake Sanabria at those times. Pollen data from lacustrine records
519 close to Lake Sanabria indicate the predominance of steppic vegetation in non-glaciated
520 neighbouring areas in response to cold and/or drier conditions at these times (Allen *et*
521 *al*., 1996; Muñoz-Sobrino *et al*., 2004). Starting towards the end of the LGM at ~19 cal
522 ka BP (e.g. upper part of Unit 3), the progressive trend toward larger C/N values
523 suggests a gradual, yet subtle appearance of vegetation in the catchment of Lake
524 Sanabria. This process involved a decrease in the relative importance of glacial grinding
525 and the onset of pedogenic processes in the catchment. Since the grain size of Paleozoic
526 rocks from the catchment of Lake Sanabria is very coarse (Fig. 2), this resulted in the
527 production of progressively coarser grained sediments as indicated by decreasing Rb/Zr
528 ratios. Deglaciation was likely punctuated by short-lived periods at around 19, 17-16
529 and 14-12.6 cal ka BP characterized by lower Rb/Zr and higher C/N ratios. The last of
530 these periods (e.g. 14-12.6 cal ka BP) lasted longer, was more prominent according to
531 the Rb/Zr and C/N ratios, and was broadly coeval with the Bølling-Allerød warm
532 interstadial. This period was accompanied by the first significant increase in TOC in the
533 lake sediments, which likely marks the onset of forest development in the catchment of
534 the lake in agreement with neighboring by pollen records (Allen *et al*., 1996; Muñoz-
535 Sobrino *et al*., 2004). This is the main phase of glacial retreat in the Lake Sanabria
536 basin. Sediments accumulated during this period are also characterized by S-ratios as
537 low as ~0.5 (Fig. 7). The catchment rocks with the lowest S-ratios are the tuffs from the
538 Ollo de Sapo Formation, which make up only the headwaters of the Tera valley (Fig. 1).
539 We interpret that a shift toward lowest S-ratios in these lacustrine sediments indicates

that glaciers were then restricted to the headwaters of the Tera valley, so that grinding of tuffs constituted the bulk of glacial-derived material transported into the lake. If this interpretation is correct, another period of glacial retreat is identified around 19 cal ka BP, coinciding with a significant minimum in Rb/Zn and a maximum in C/N ratios. Rock magnetic data therefore support the variability in glacial dynamics reported during the proglacial stages, and also support the notion of a deglaciated basin by ca 14 cal ka BP proposed by Jambrina-Enríquez *et al*. (2014).

Glacier retreat during the Bølling-Allerød likely culminated by 12.6-12.2 cal ka BP (Jambrina-Enríquez *et al*., 2014), and it is marked by the shift to a magnetite-, maghemite- and greigite-bearing magnetic assemblage (S-ratios > 0.8 and SIRM/χ > 3 kA/m) and to low Rb/Zr (<1.5) and high TOC (>5%) values observed within Unit 2B (Fig. 7). Between 12.2 and 11 cal ka BP (e.g. Unit 2A), a prominent minimum in TOC and C/N values indicates a significant decrease in terrestrial vegetation in the lake catchment (Fig. 7). This period partly overlaps with the Younger Dryas, which is identified in neighbouring lake records by a decrease in arboreal pollen in response to cooler conditions in the region (Allen *et al*., 1996; Muñoz-Sobrino *et al*., 2004). Lowest Rb/Zr ratios between 12.2 and 11 cal ka BP suggest deposition of coarse silts and fine sands, likely in response to colder conditions in which freeze-thaw processes in the highlands dominate sediment production. The lack of pyrrhotite in sediments accumulated during this period, coupled with the dominance of magnetite and the occurrence of maghemite and greigite, suggests the dominance of pedogenic processes and minimal glacial grinding in the catchment of the lake. The absence of a magnetic glacial signature during this interval suggests a minimal re-activation of glaciar processes (grinding, flour transport) during the Younger Dryas. ARM values during this period are above those of catchment rocks (Fig. 4), which attest to significant pedogenic

565 activity in the catchment of the lake and to the arrival of soil-derived material to the
566 lake. Since magnetite, maghemite and greigite all contribute to the ARM, it is not
567 possible to discern whether increased inputs of detrital magnetic minerals or enhanced
568 authigenic formation of greigite dominate the signal. Since authigenic greigite growth
569 was triggered by the input of terrestrial organic matter into the lake, it is likely that both
570 enhanced terrigenous supply and diagenesis operated in concert.

571 Between 11 and ~3 cal ka BP (e.g. Units 1E to 1B), low Rb/Zr ratios and high TOC
572 and C/N values dominate the record (Fig. 7). Although ARM values and S-ratios are
573 slightly lower during this period, they are still significantly larger than those of
574 catchment rocks (Fig. 4). This suggests slightly decreased, yet stable background
575 pedogenic activity, terrigenous supply and diagenetic conditions. The most remarkable
576 features during this period are two distinctive intervals at 10 and 7.4 cal ka BP, which
577 correspond to prominent light colored sandy layers that are characterized by
578 geochemical (Rb/Zr, TOC, C/N) and magnetic (S-ratios, ARM and SIRM/χ) properties
579 typical of sediments accumulated before the deglaciation (Fig. 7). We interpreted that
580 these layers derived from glacial-derived material stored in the Quaternary tills that crop
581 out in the catchment of Lake Sanabria, which provided the main source of sedimentary
582 input during periods of extreme runoff conditions. These two main periods of increased
583 river input are in agreement with European records at similar latitudes and are
584 synchronous with cold and humid events described at 10.1 and 7.5 cal ka BP in the
585 North Atlantic (see Jambrina-Enríquez *et al*., 2014). Runoff events were more frequent,
586 albeit with a smaller significance and giving way to thinner (mm-scale) silt layers,
587 during deposition of Unit 1E between 10.4 and 7 cal ka BP (Figs. 3 and 7), likely
588 associated with a negative NAO mode-like (Jambrina-Enríquez *et al*., 2014).
589 Noticeably, no major change in sedimentary dynamics is identified that could be

590 associated to the 8.2 kyr cooling event in the North Atlantic despite the strong influence
591 of Atlantic climate variability in the Lake Sanabria region and the recognition of the 8.2
592 kyr event in other Northern Iberian continental records (Gómez-Paccard *et al*., 2013).

593 At around 3 cal ka BP, a significant increase in S-ratios and ARM values and a
594 gradual rise in SIRM/χ values are observed while geochemical parameters remain rather
595 stable (Fig. 7). These variations likely reflect enhanced detrital inputs and diagenesis
596 operating in concert, and appear to mark an increase in non-arboreal pollen associated
597 with the onset of human-induced deforestation that prevails throughout the rest of the
598 record until the present (Muñoz-Sobrino *et al*., 2004).

599

600 **6. Conclusions**

601 The source-to-sink environmental magnetic study of a Late Pleistocene-holocene
602 sediment core from Lake Sanabria and from different rocks of its catchment
603 complements previous sedimentological and geochemical studies, and therefore gives
604 new insights on the climatic evolution of the NW Iberian Peninsula during the last
605 deglaciation. Our results indicate that the magnetic assemblage of sediments from the
606 lower half of the studied sequence, accumulated between ~26 and ~13 ka BP in a
607 proglacial environment, and of the Paleozoic rocks that make up most of the catchment
608 of the lake, is characterized by magnetite and, likely also, pyrrhotite. The occurrence of
609 these minerals both in the catchment rocks and in the lake sediments indicates that
610 sedimentation was then driven by the erosion of glacial flour, which suffered minimal
611 chemical transformation in response to a rapid and short routing to the lake. Sediments
612 from the upper half of the studied sequence, accumulated after 12.6 ka BP in a
613 lacustrine environment with strong fluvial influence, contain magnetite and smaller

amounts of maghemite and greigite. These findings point to a significant role of post-depositional reducing conditions once the sediments were accumulated in the lake, but also to a significant imprint of pedogenic activity in the lake catchment before detrital material was transported into the lake. The sharp change in magnetic properties observed in the lake sediments between 13 and 12.6 ka BP, coupled to more subtle changes in rock magnetic data at ca 14 cal ka BP, supports the rapid deglaciation of the catchment of Lake Sanabria inferred in previous studies on the basis of sedimentological, geochemical and geomorphological data.

Acknowledgements

The research has been funded by the Spanish Ministry of Science and Competitiveness (CONSOLIDER – GRACCIE Project), the Fundación Patrimonio Natural de Castilla y León, and a Marie Curie Intra European Fellowship IEF-2012 (MGP). We are grateful to the Paleomagnetic Laboratory CCiTUB-ICTJA CSIC and the Magnetic Fabric Laboratory at the University of Zaragoza for their support and technical assistance with rock magnetic experiments, and to Qingsong Liu for his assistance with interpretation of thermomagnetic runs.

References

Aldasoro JJ, de Hoyos C, Vega JC, 1991. *El lago de Sanabria. Estudio Limnológico.* Publicaciones Monográficas de la Red de Espacios Naturales de Castilla y León. Consejería de Medio Ambiente y Ordenación del Territorio, 2. Dirección General del Medio Ambiente, Valladolid, Spain.

637 Allen JRM, Huntley B, Watts WA, 1996. The vegetation and climate of northwest
638 Iberia over the last 14000 yr. *Journal of Quaternary Science* **11**: 125–147.

639 Bloemendal J, King JW, Hall FR, Doh S-J, 1992. Rock magnetism of late Neogene and
640 Pleistocene deep-sea sediments: Relationship to sediment source, diagenetic
641 processes, and sediment lithology. *Journal of Geophysical Research* **97**: 4361–4375,
642 doi:10.1029/91JB03068.

643 Cowton T, Highes PD, Gibbard PL, 2009. Palaeoglaciation of Parque Natural Lago de
644 Sanabria, northwest Spain. *Geomorphology* **108**, 282–291.

645 de Hoyos C., 1996. *Limnología del Lago de Sanabria: variabilidad interanual del*
646 *fitoplancton*. Unpublished PhD Thesis. Universidad de Salamanca, 438 pp.

647 de Hoyos C, Aldasoro JJ, Toro M, Comín FA, 1998. Specific composition and ecology
648 of chrysophyte flagellates in Lake Sanabria (NW Spain). *Hidrobiologia* **369/370**:
649 287–295.

650 de Hoyos C, Comín FA, 1999. The importance of inter-annual varibility for
651 management. *Hydrobiologia* **395–396**: 281–291.

652 Dearing J, Hu YQ, Doody P, James AP, Brauer A, 2001. Preliminary reconstruction of
653 sediment-source linkages for the past 6000 yr at the Petit Lac d´Annecy, France,
654 based on mineral magnetic data. *Journal of Paleolimnol*ogy **25**: 245–258.

655 Dergachev VA, Raspopov OM, Damblon F, Jungner H, Zaitseva GI, 2007. Natural
656 climate variability during the Holocene. *Radiocarbon* **49**: 837–854.

657 Dekkers MJ, 1989. Magnetic properties of natural pyrrhotite. II. High- and low-
658 temperature behaviour of *Jrs* and TRM as function of grain size. *Physics of the Earth*
659 *and Planetary Interiors* **57**: 266–283.

660 Dunlop DJ, Özdemir Ö, 1997. *Rock Magnetism, Fundamentals and Frontiers.*
661 Cambridge Univ. Press, Cambridge, U.K.

662 Dypvik H, Harris NB, 2001. Geochemical facies analysis of fine-grained siliciclastics
663 using Th/U, Zr/Rb and (Zr+Rb)/Sr ratios. *Chemical Geology* **181**: 131–146.

664 Evans ME, Heller F, 2003. *Environmental magnetism. Principles and applications of*
665 *environmagnetics*. Academic, San Diego, Calif., 299 pp.

666 Giorgio F, Lionello P, 2008. Climate change projections for the Mediterranean region.
667 *Global and Planetary Change* **63**: 90–104.

668 Giralt S, Rico-Herrera MT, Vega JC, Valero-Garcés B, 2011. Quantitative climate
669 reconstruction linking meteorological, limnological and XRF core scanner datasets:
670 the Lake Sanabria case study, NW Spain. *Journal of Paleolimnol*ogy **46**: 487–502.

671 Gómez-Paccard M, Larrasoaña JC, Sancho C, Muñoz A, McDonald E, Rhodes EJ,
672 Osácar MC, Costa E, Beamud. E, 2013. Environmental response of a fragile,
673 semiarid landscape (Bardenas Reales Natural Park, NE Spain) to Early Holocene
674 climate variability: A paleo- and environmental-magnetic approach. *Catena* **103**: 30–
675 43.

676 Horng CS, Roberts AP, 2006. Authigenic or detrital origin of pyrrhotite in sediments?:
677 Resolving a paleomagnetic conundrum. *Earth and Planetary Science Letters*
678 **241**:750–762.

679 Jalut G, Turu i Michels V, Dedoubat JJ, Otto T, Ezquerra J, Fontugne M, Belet JM,
680 Bonnet L, García de Celis, AG, Redondo-Vega JM, Vidal-Romaní JR, Santos L,
681 2010. Palaeoenvironmental studies in NW Iberia (Cantabrian range): Vegetation

682 history and synthetic approach of the last deglaciation phases in the western
683 Mediterranean. *Palaeogeography, Palaeoclimatology, Palaeoecology* **297**: 330–350.

684 Jambrina-Enríquez M, Rico M, Moreno A, Leira M, Bernárdez P, Prego R, Recio C,
685 Valero-Garcés B, 2014. Timing of deglaciation and postglacial environmental
686 dynamics in NW Iberia: the Sanabria Lake record. *Quaternary Science Reviews* ***94:***
687 *136-158.*

688 Jiménez-Sánchez M, Farias P, Arquer P, 2002. New radiometric and geomorphological
689 evidence of last glacial maximum older than 18 ka in SW European mountains: the
690 example of Redes Natural Park (Cantabrian Mountains, NW Spain). *Geodinamica*
691 *Acta* **15**, 93–101.

692 Jiménez-Sánchez M, Rodríguez-Rodríguez L, García-Ruiz JM, Domínguez-Cuesta MJ,
693 Farias P, Valero-Garcés B, Moreno A, Rico M, Valcárcel M., 2012. A review of
694 glacial geomorphology and chronology in northern Spain: Timing and regional
695 variability during the last glacial cycle. *Geomorphology* **196**: 50–64.

696 Julià R, Luque JA, Siera S, Alejandro JA, 2007. Climatic and land use changes on the
697 NW of Iberian Peninsula recorded in a 1,500-year record from Lake Sanabria.
698 *Contribution to Science* **3**: 355–369.

699 Larrasoaña JC, Roberts AP, Musgrave RJ, Gràcia E, Piñero E, Vega M., Martínez-Ruiz
700 F, 2007. Diagenetic formation of greigite and pyrrhotite in gas hydrate marine
701 sedimentary systems. *Earth and Planetary Science Letters* **261**: 350–366.

702 Last, WM, Smol JP, 2001. *Tracking environmental change change using lake sediments.*
703 *Volume 1: Basin Analysis, Coring, and Chronological Techniques*. Springer.

704 Liu Q, Deng C, Yu Y, Torrent J, Jackson MJ, Banerjee SK, Zhu R, 2005. Temperature
705 dependence of magnetic susceptibility in an argon environment: implications for
706 pedogenesis of Chinese loess/palaeosols. *Geophysical Journal International* **161**:
707 102–112.

708 Liu Q, Roberts AP, Larrasoaña JC, Banerjee SK, Guyodo Y, Tauxe L, Oldfield F, 2012.
709 Environmental magnetism: principles and applications. *Reviews of Geophysics* **50**:
710 RG4002, doi:10.1029/2012RG000393.

711 Lowrie W, 1990. Identification of ferromagnetic minerals in a rock by coercivity and
712 unblocking temperature properties. *Geophysical Research Lett*ers **17**: 159–162.

713 Martínez-García, E., 1973. Deformación y metamorfismo en la zona de Sanabria
714 (provincias de Zamora, León y Orense, noroeste de España). *Estudios Geológicos*. **5**:
715 7–106.

716 Moreno A, Valero-Garcés BL, Jiménez-Sánchez M, Domínguez MJ, Mata P, Navas A,
717 González-Sampériz P, Stoll H, Farias P, Morellón M, Corella P, Rico M, 2010. The
718 last deglaciation in the Picos de Europa National Park (Cantabrian Mountains,
719 Northern Spain). *Journal of Quaternary Science* **25**: 1076–1091.

720 Muñoz-Sobrino C, Ramil-Rego P, Gómez-Orellana L, 2004. Vegetation of the Lago de
721 Sanabria area (NW Iberia) since the end of the Pleistocene: A palaeoecological
722 reconstruction on the basis of two new pollen sequences. *Vegetation History and*
723 *Archaebotany* **13**: 1–22.

724 Negro A.I., de Hoyos C., Vega J.C., 2000. Phytoplankton structure and dynamics in
725 Lake Sanabria and Valparaíso reservoir (NW Spain). *Hydrobiologia* **424**: 25–37.

726 Oldfield F, 2013. Mud and magnetism: Records of late Pleistocene and Holocene
727 environmental change recorded by magnetic measurements. *Journal of*
728 *Paleolimnology* **49**: 465–480.

729 O'Reilly WO, Hoffmann V, Chouker AC, Soffel HC, Mennyeh A, 2000. Magnetic
730 properties of synthetic analogues of pyrrhotite ore in the grain size range 1-24 μm.
731 *Geophysical Journal International* **142**: 669–683.

732 Pérez-Estaún, A., Bea F., 2004. *Macizo Ibérico*. In: Geología de España (Vera JA, ed.).
733 SGE-IGME, Madrid, 19–228.

734 Peters C, Dekkers MJ, 2003. Selected room temperature magnetic parameters as a
735 function of mineralogy, concentration and grain size. *Physics and Chemistry of the*
736 *Earth* **28**: 659–667.

737 Roberts AP, Weaver R, 2005. Multiple mechanisms of remagnetization involving
738 sedimentary greigite (Fe3S4). *Earth and Planetary Science Letters* **231**: 263–277.

739 Roberts AP, Chang L, Rowan CJ, Horng CS, Florindo F, 2011. Magnetic properties of
740 sedimentary greigite (Fe_3S_4): An update. *Reviews of Geophysics* **49**: RG1002,
741 doi:10.1029/2010RG000336.

742 Rodríguez-Rodríguez L, Jiménez-Sánchez M, Domínguez-Cuesta MJ, Rico MT,
743 Valero-Garcés B, 2011. Last deglaciation in northwestern Spain: New chronological
744 and geomorphologic evidence from the Sanabria region. *Geomorphology* **135**: 48–
745 65.

746 Rodríguez-Rodríguez L, Jiménez-Sánchez M, Domínguez-Cuesta MJ, Rinterknecht V,
747 Pallàs R, Valero-Garcés B, 2014. A multiple dating-method approach applied to the
748 Sanabria Lake moraine complex (NW Iberian Peninsula, SW Europe). *Quaternary*
749 *Science Reviews* **83**, 1–10.

750 Rosenbaum JG, Reynolds RL, 2004. Basis for paleoenvironmental interpretation of
751 magnetic properties of sediment from Upper Klamath Lake (Oregon): effects of
752 weathering and mineralogical sorting. *Journal of Paleolimnology* **31**: 253–265.

753 Schnurrenberger D, Russell J, Kelts K, 2003. Classification of lacustrine sediments
754 based on sedimentary components. *Journal of Paleolimnology* **29**: 141–154.

755 Snowball I.F, 1991. Magnetic hysteresis properties of greigite (Fe_3S_4) and a new
756 occurrence in Holocene sediments from Swedish Lappland. *Physics of the Earth and*
757 *Planetary Interiors* **68**: 32–40, doi:10.1016/0031-9201(91)90004-2.

758 Thompson R, Oldfield F, 1986. *Environmental Magnetism*. Allen and Unwin,
759 Winchester, Mass.

760 Vega JC, de Hoyos C, Aldasoro JJ, 1991. *Estudio del sistema de lagunas de las sierras*
761 *Segundera y Cabrera*. In: Monografías de la red de Espacios naturales de Castilla y
762 León, Junta de Castilla y León, Consejería de Medio Ambiente y Ordenación del
763 Territorio, Valladolid, Dirección general del Medio Natural.

764 Vega JC, de Hoyos C, Aldasoro JJ, 1992. The Sanabria Lake: the largest natural
765 freshwater lake in Spain. *Limnetica* **8**: 49–57.

766 Vega JC, Aldasoro JJ, 1994. *Geología de Sanabria*. In: Monografías de la Red de
767 Espacios Naturales de Castilla y León, Consejería de Medio Ambiente y Ordenación
768 del Territorio (Junta de Castilla y León), Valladolid.

769 Vega JC, Hoyos C, Aldasoro JJ, de Miguel J, Fraile H, 2005. Nuevos datos
770 morfométricos para el Lago de Sanabria. *Limnetica* **24**: 115–122.

771

772 **Figure captions:**

773 Figure 1. Location and geological sketch map of the Lake Sanabria region. Core
774 SAN04-3A-1K sampling site (blue circle) and block-samples sampling locations (red
775 dots) are indicated. Modified from Rodríguez-Rodríguez *et al*. (2011).

776

777 Figure 2. Field and hand sample pictures of the main lithologies that constitute the
778 catchment of Lake Sanabria. (a, b) Schists of the Puebla Formation (c, d) Gneisses of
779 the Ollo de Sapo Formation (e, f) Granites emplaced within the gneisses, (g) Schists of
780 the Puebla Formation, (h) Quaternary tills.

781

782 Figure 3. Downcore variations of selected physical and geochemical properties of
783 sediments from core SAN04-3A-1K (TOC, C/N, Rb/Zr; Jambrina-Enríquez *et al*.,
784 2014), along with our rock magnetic data (χ, HIRM, ARM, χ_{ARM}/SIRM and SIRM/χ).
785 The AMS calibrated dates, the sedimentary log and the interpretation of sedimentary
786 environment are after Jambrina-Enríquez *et al*. (2014). Notice that Rb/Zr ratios are
787 plotted in reverse order. Asterisks indicate the position of samples selected for rock
788 magnetic experiments.

789

790 Figure 4. Bi-plot of (a) S-ratio versus ARM (Am^2/kg) and (b) SIRM/χ (kA/m) for
791 samples from core SAN04-3A-1K and for the rocks collected in the catchment area of
792 Lake Sanabria.

793

794 Figure 5. Representative examples of thermal demagnetization of three-axis isothermal
795 remanent magnetization. Results from core SAN04-3A-1K sediments and from
796 different rocks collected in the catchment area of Lake Sanabria are showed.
797
798 Figure 6. Thermomagnetic runs for representative samples from core SAN04-3A-1K
799 sediments and from different rocks collected in the catchment area of Lake Sanabria.
800 Notice the different scale associated to the warming (in red) and cooling (in blue)
801 curves. Dashed vertical bars indicate temperature intervals of features discussed in the
802 text.
803
804 Figure 7. Age variations of selected geochemical and rock magnetic properties of
805 sediments from core SAN04-3A-1K. Notice that Rb/Zr ratios are plotted in reverse
806 order.
807

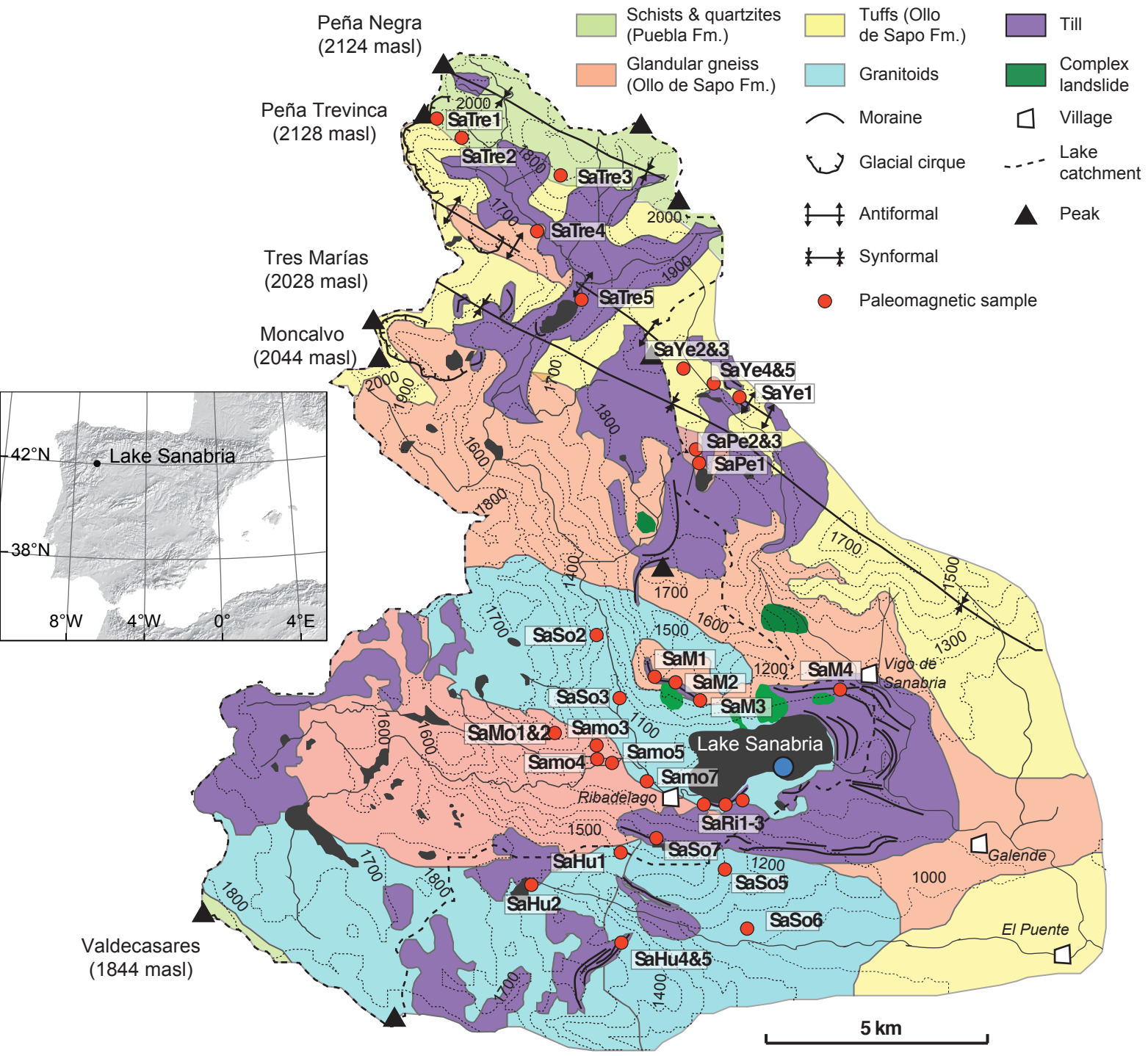

Figure 1
Borruel et al

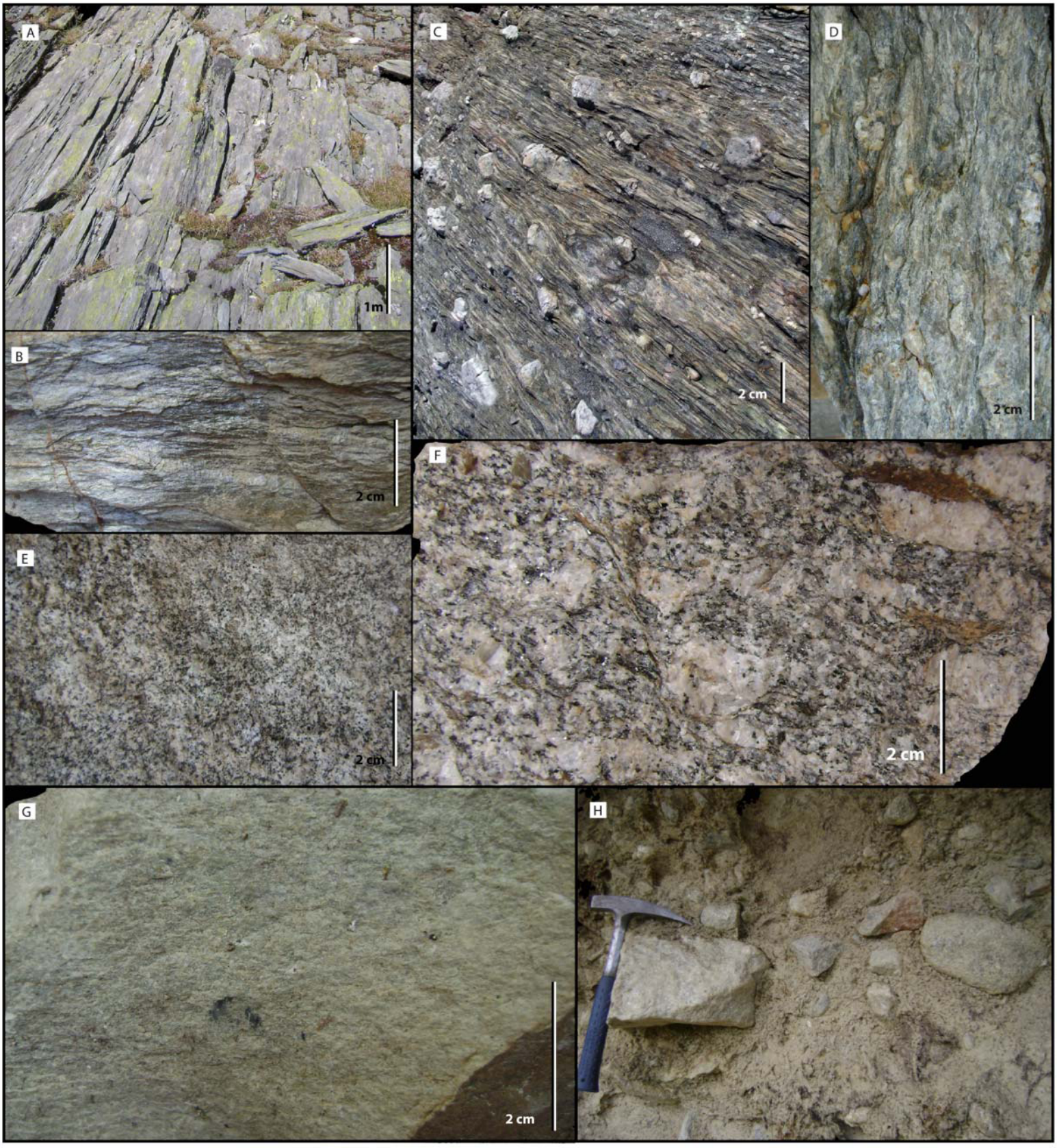

Figure 2
Borruel et al

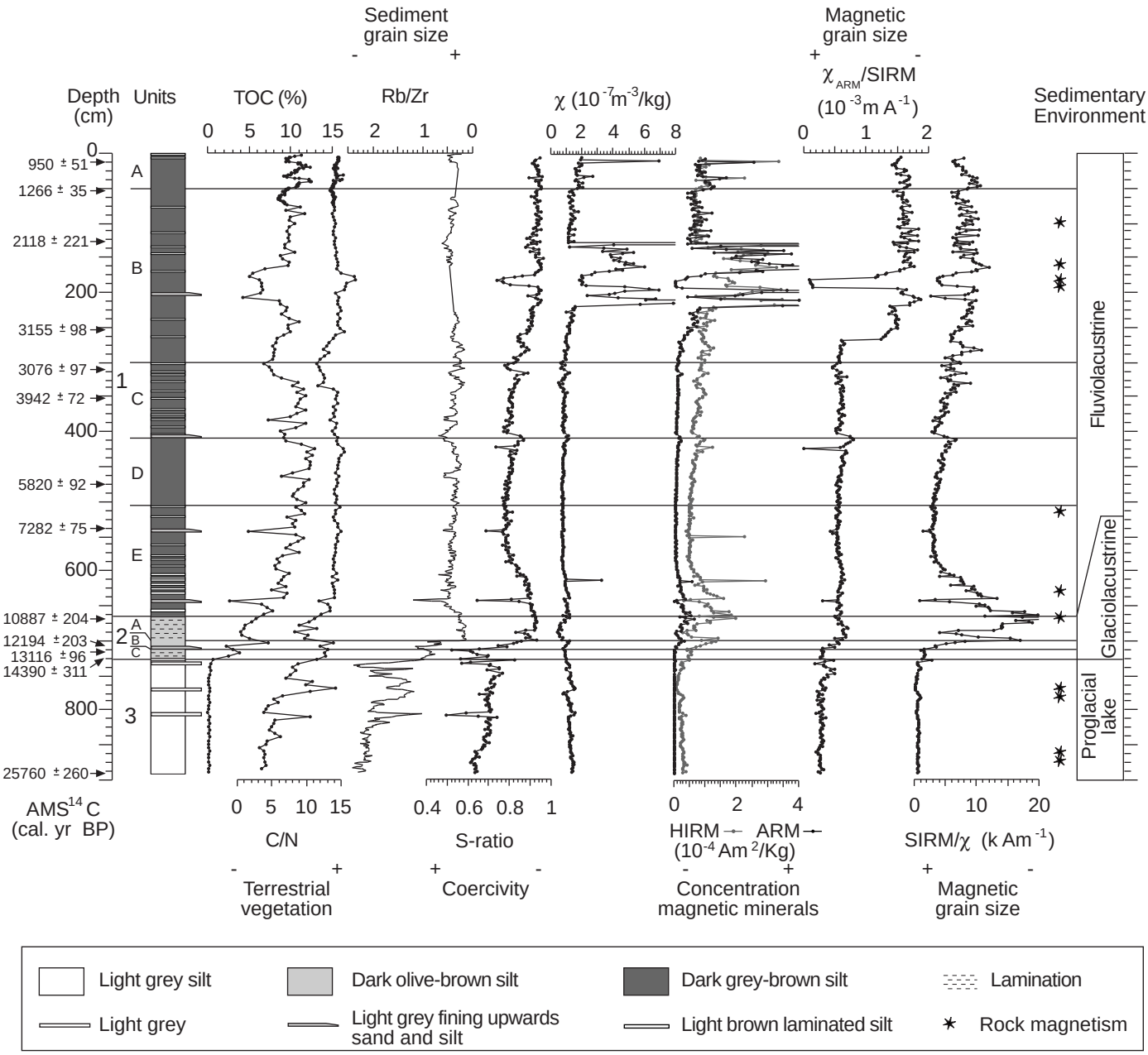

Figure 3
Borruel et al.

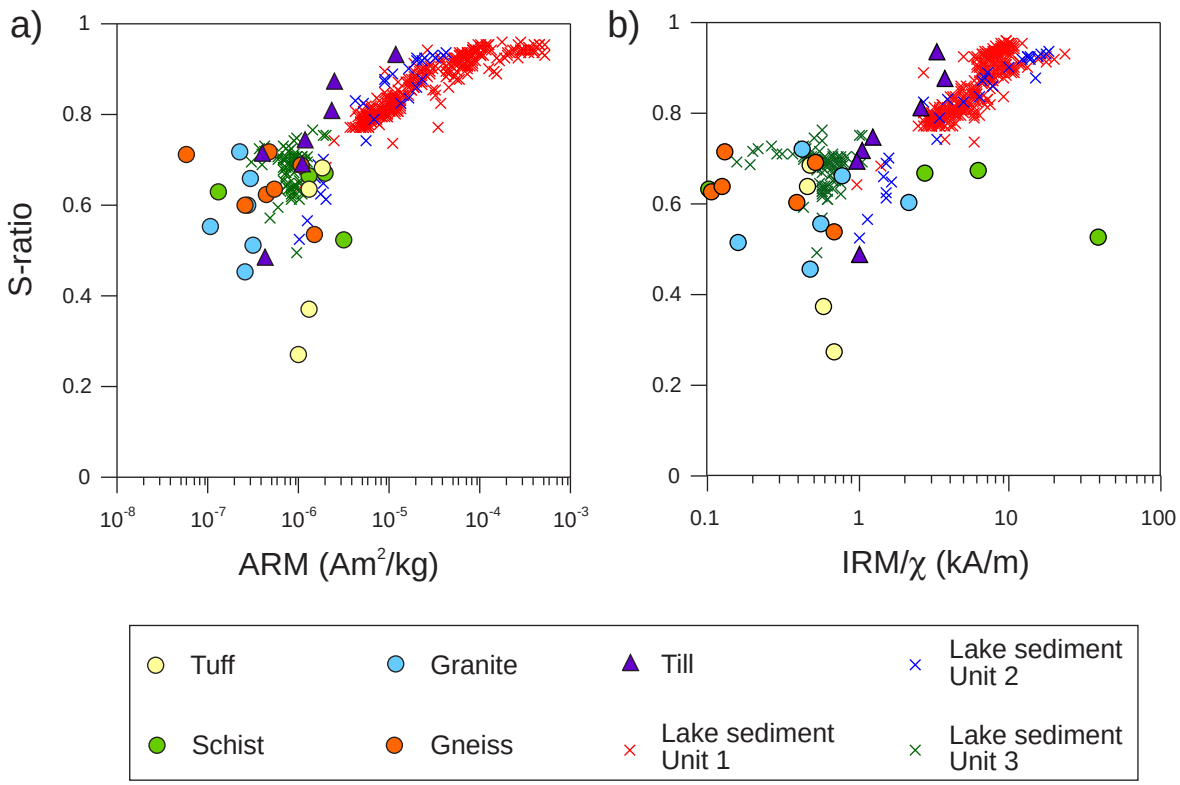

Figure 4
Borruel et al.

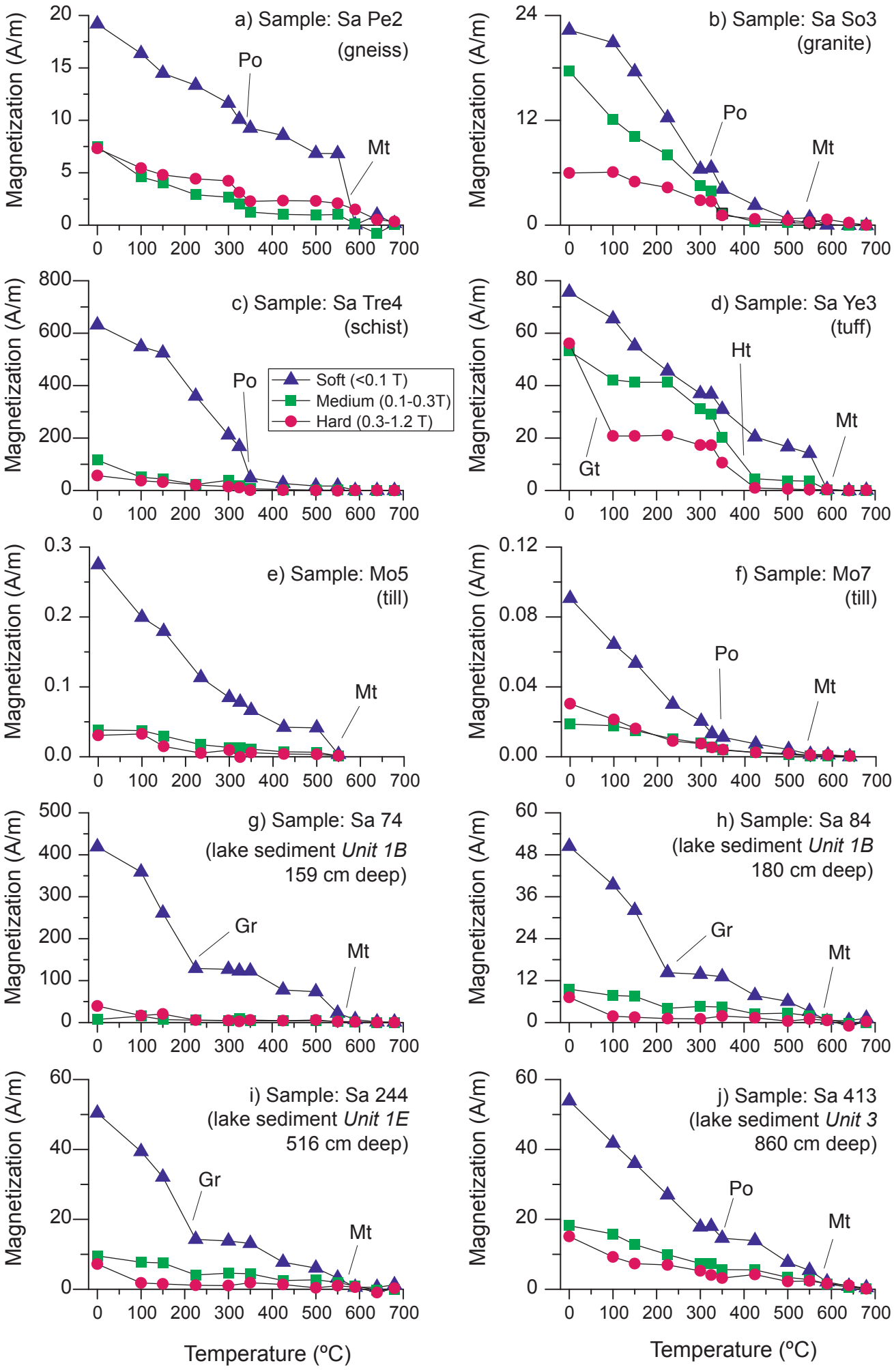

Figure 5
Borruel et al

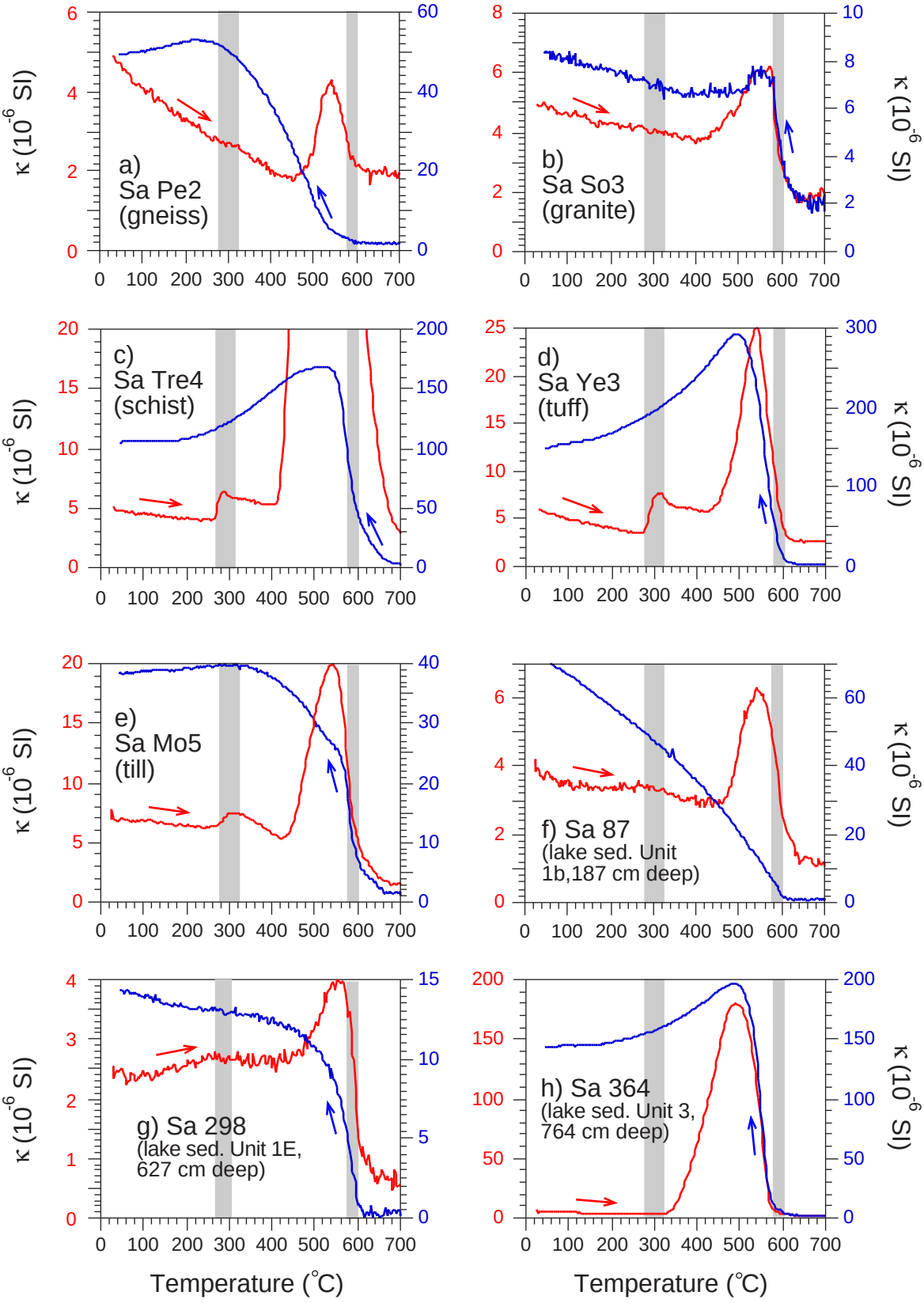

Figure 6
Borruel et al.

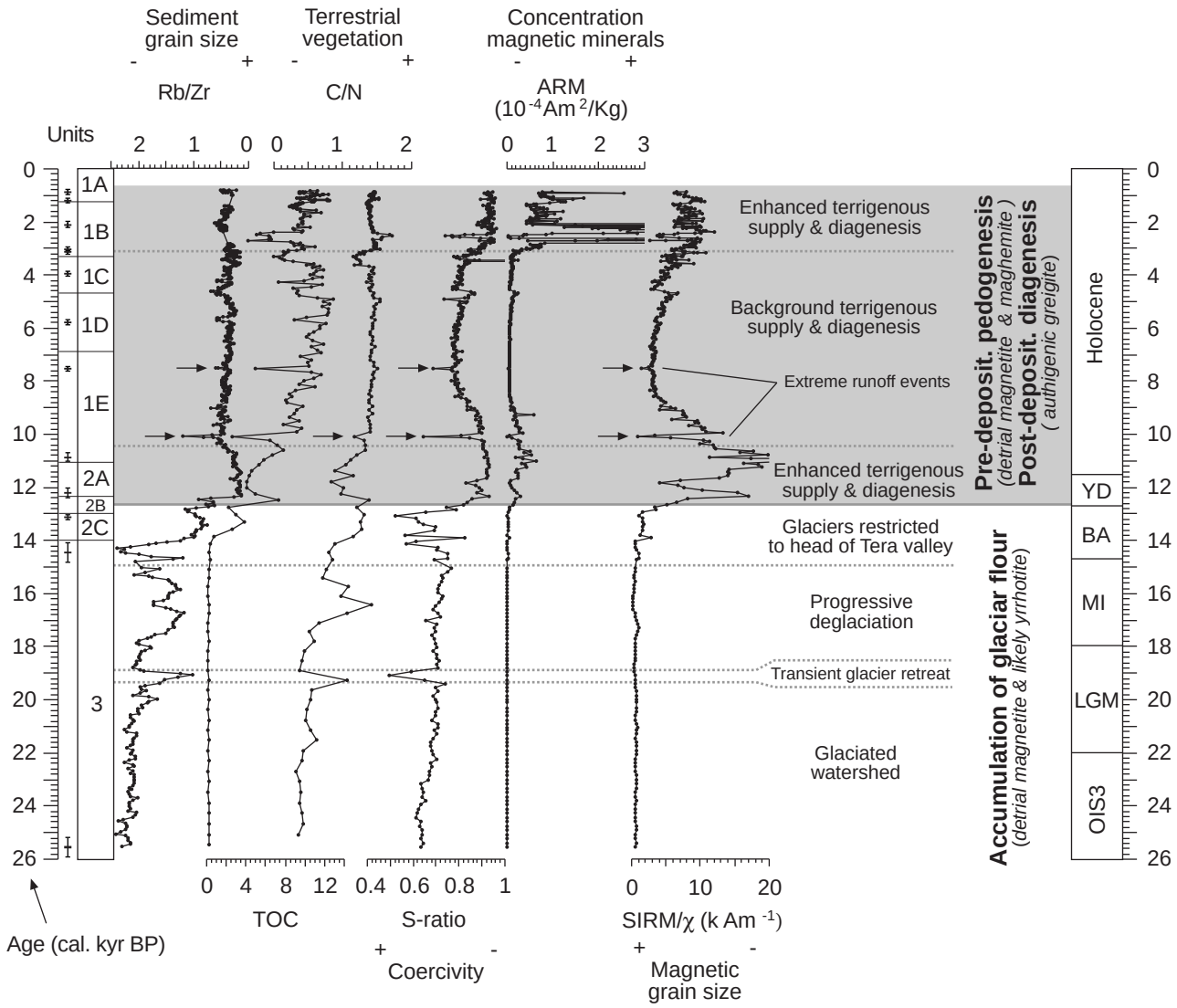

Figure 7
Borruel et al.